Santa Clara University
Scholar Commons

6-2022

Shear Detection of Microencapsulated Cells for Monoclonal Antibody Production Scaleup

Kendall Defelippi

Dwight Johnson

SANTA CLARA UNIVERSITY

Department of BioEngineering

I HEREBY RECOMMEND THAT THE THESIS PREPARED
UNDER MY SUPERVISION BY
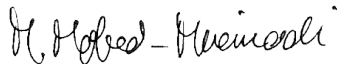
Kendall Defelippi, Dwight Johnson

ENTITLED

SHEAR DETECTION OF MICROENCAPSULATED CELLS FOR MONOCLONAL ANTIBODY PRODUCTION SCALEUP

BE ACCEPTED IN PARTIAL FULFILLMENT OF THE REQUIREMENTS
FOR THE DEGREE OF

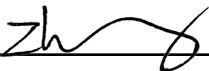**BACHELOR OF SCIENCE**
IN
BIOENGINEERING

_____   06/10/2022
Thesis Advisor(s) (use separate line for each advisor)   date

_____   06/10/2022
Department Chair(s) (use separate line for each chair)   date

SHEAR DETECTION OF MICROENCAPSULATED CELLS FOR MONOCLONAL ANTIBODY PRODUCTION SCALEUP

By

Kendall Defelippi, Dwight Johnson

SENIOR DESIGN PROJECT REPORT

Submitted to
the Department of BioEngineering

of

SANTA CLARA UNIVERSITY

in Partial Fulfillment of the Requirements
for the degree of
Bachelor of Science in BioEngineering

Santa Clara, California

2022

Acknowledgements

Our group would like to offer thanks to those who supported our senior design project: SCU School of Engineering and Department of Bioengineering for the funds and resources to complete this project. Members of Dr. Zhang's lab and Dr. Emily Park for providing us with CHO cells and cell culture materials throughout the year, as well as support maintaining our CHO cells. Ally Kwong for assisting and supporting our 3D printing efforts.

And finally, a special thank you to our advisor Dr. Mobed-Miremadi who was always willing and available to meet with us and offer guidance as we worked to complete this project. Her commitment to our success was invaluable, and we cannot thank her enough for her support.

TABLE OF CONTENTS

List of Figures

List of Tables

Chapter 1: Introduction

The introduction chapter will provide background for our project in the bioengineering field along with a review of the current field involving hydrogel formation, cell encapsulation and microneedle creation through 3D printing. In addition, there will be an overview of the various biological and technical components of our project. All of which are vital for the complete comprehension of our project and goals.

1.1 Background

Our project focuses on bioprocessing, which is a process that translates biological resources, such as mammalian cells into useful industrial products [1]. One of the many therapies created using bioprocessing are monoclonal antibodies [2]. Currently, there is a huge need for large scale production of monoclonal antibodies to treat cancer, Covid-19, and other diseases [3],[4].

Bioprocessing typically takes place in industrial bioreactors, which produce standardized, reproducible cell based therapies on a large scale [5]. There are a wide variety of bioreactors, ranging in size from 15 mL to 2000 L. Industrial bioreactors are extremely high throughput, however they do cause cell damage by inducing hydrodynamic stress [6]. This excess hydrodynamic stress leads to cell death and reversion, but it is difficult to quantify this stress between scales [7],[8]. Therefore, there is a need to develop strategies to analyze hydrodynamic stress on the small scale so that hydrodynamic stress can be understood during the scaleup process.

Our project builds upon the work of a 2018 senior design project titled "Three-Dimensional (3D) Printed Microneedles for Microencapsulated Cell Extrusion" [9]. The main objective of this project was to create a hollow microneedle and identify the optimum flow rate for the extrusion of viable encapsulated cells through a microneedle array for wound healing applications. This project highlights the feasibility of encapsulated cell extrusion, specifically protection from shear, through a hollow microneedle assembly, as there were very low values of hydrodynamic stress (~ 1 Pa) associated with extrusion through their device. For our project, we will be creating a soft sensor device for bioprocessing by redesigning the wound healing microneedle

1

device to induce more shear and be used as a prescreening tool for bioprocessing applications.

Table 1. Background and Inspiration Behind Project

	2018 SD [9]	2020 Industrial Grant	2021 SD [10]	2022 SD
Translation	Wound healing	Industrial bioprocessing problem statement identified	Simulation	Bioprocessing of **shear**
Biomaterials	U87 cells, alginate, polymethyl methacrylate (PMMA)	N/A	N/A	**Chinese Hamster Ovary (CHO) cells**, 3% alginate, PMMA
Device	3D printing, stereolithography (SLA)	N/A	N/A	3D printing, SLA, **design change**
Biocompatibility Testing	WST-1 Cytotoxicity Assay [11]	N/A	N/A	**Lactate dehydrogenase (LDH)** cytotoxicity assay
Computation	N/A	Statistical Proof of Shear	Fracture, clogging, shear **(CAD/CAM)**	Increased **hydrodynamic shear**

1.2 Problem Statement

The goal of our project is to design a soft biosensor device for detecting hydrodynamic shear in microencapsulated cells prior to each scale-up step during bioprocessing.

1.3 Review of Field

1.3.1 Hollow Microneedle Arrays

Generally, microneedle types can be separated into four categories (Figure 1): solid, coated, dissolving, and hollow [12]. Our project focuses on the use of hollow microneedles, which are like hypodermic needles, but are shorter in length. Most research and applications of hollow microneedle arrays involve transdermal drug delivery. The use of microneedles for transdermal

2

drug delivery are advantageous over traditional dermal patches, as the dermal patch cannot deliver drugs through the top layer of the skin if they are not lipid-soluble [13]. Additionally, microneedles have the ability to pierce through the stratum corneum and enter the desired delivery site of the skin layers in a minimally-invasive method [14].
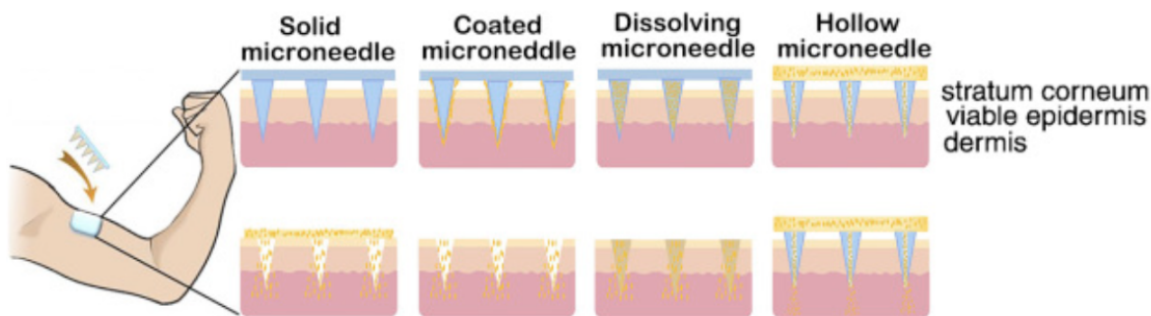
Figure 1. Methods of transdermal drug delivery using solid, coated, dissolving, and hollow microneedle patches [12].

For wound healing applications, it is important that shear stress is limited so that the encapsulated cells survive and are delivered properly to the skin through the microneedle array. This means that many microneedle array systems aim to decrease the amount of shear stress experienced by the cells during delivery [15]. In the case of our project, we want to maximize the shear stress experienced by encapsulated cells in order to mimic the environment of industrial bioreactors.

1.3.2 Bioprocessing of Shear

As mentioned previously, high levels of shear stress are associated with bioprocessing. In the bioreactor environment, cells can be damaged by high shear stress, tearing apart cells and cell aggregates and resulting in lower cell quality and cell yield [16]. Additionally, current studies show that there exists a lack of scalable protocols for the inoculation and harvesting phases

[17],[18]. Therefore, there is a need to develop strategies to analyze hydrodynamic stress on the small scale so that hydrodynamic stress can be understood during the scaleup process.

1.4 Biological and Technical Components

1.4.1 Biomaterials

The purpose of cell encapsulation technologies is to trap viable and functional cells within a semipermeable matrix [19]. There are a variety of different materials that can be used for cell encapsulation. Common carbohydrates used for cell encapsulation include agarose, chitosan, and alginate, while common proteins used for microencapsulation include collagen, gelatin, and elastin [19]. Our project will utilize alginate, which is the most widely used material for the encapsulation of living cells [20]. Alginate capsules will be created using $CaCl_2$, which is one of the most commonly used agents to ionically crosslink alginate [20].

Viscoelasticity is an important component of alginate hydrogels, as the physical properties of the extracellular matrix affect cell behaviors such as cell adhesion and migration to differentiation [21]. Recent studies have revealed ECM viscoelasticity, independent of stiffness, as a critical physical parameter regulating cellular processes, such as cell spreading [22],[23]. These properties are important to consider when creating alginate capsules.

Another biomaterial associated with our project is polymethyl methacrylate (PMMA). PMMA is a transparent, lightweight thermoplastic resin that is synthesized by polymerizing methyl methacrylate [24]. PMMA is a biocompatible material [25] and will be used when 3D printing our soft biosensor.

1.4.2 Cells

There are a multitude of different mammalian cell lines. Our project uses Chinese Hamster Ovary (CHO) cells, as CHO cells have become the standard mammalian host cell line and are often used for commercial manufacturing [26]. CHO cells have been proven to be easy to culture, have FDA-approval, and have low susceptibility to viruses [26],[27]. CHO cells also can grow in serum-free and chemically defined media, ensuring reproducibility between different batches of cell culture [27].

1.4.3 3D Printing

Our project utilizes stereolithography (SLA), a 3D printing process that uses a UV laser to cure liquid photoresin by free radical polymerization into hardened plastic [28]. The process involves a computer-controlled UV laser beam, which has been pre-programmed using CAM/CAD software, to draw a cross-section of the 3D model and selectively harden the material with the print being built in consecutive layers. Inverted stereolithography is the most common SLA system, and is the system that is utilized in our lab. Inverted SLA is popular because it requires a much smaller resin tank compared to build volume [29]. Additionally, the creation of upside-down machines allowed stereolithography to move to the desktop, with a smaller footprint and much lower cost [29]. Finally, SLA has a maximum resolution at 25 um [30], making it an ideal 3D printing method to use when creating designs on the millimeter or micron scale.

1.4.4 Bioreactors

Bioreactors are engineered systems that are used to maintain well-controlled microenvironments that regulate cell growth, differentiation, and tissue formation [31]. Bioreactors are extremely important in the cell-based therapy industry, as they are necessary in order to produce standardized, reproducible cell based products for regenerative medicine applications [31]. Additionally, bioreactors are advantageous because large numbers of cells (10^8 to 10^{10}) are needed in order for cell-based therapies to be effective and successful [31]. This means that a large amount of space is needed to grow the cells in a way that the standard cell culture apparatus is not able. Because bioreactors are able to support industrial-scale, ultra-high-density cell suspension cultures with controlled microenvironments, standardization, and uniformity of culture conditions, these systems are important tools for the large-scale production of cell therapies.

There are three main classes of bioreactors: cell expansion bioreactors, tissue engineering bioreactors, and lab-on-a-chip systems [31]. In our project, we will be focusing on cell expansion bioreactors. Cell expansion bioreactors are important because of the necessity to produce large quantities of high quality therapeutics in the biotechnology industry [32]. There are a variety of factors that are crucial to the scaleup process, such as mixing time, oxygen transfer, and carbon dioxide removal [32]. Specifically, one study found that scaling up to a 5,000 L bioreactor led to

a lower oxygen transfer coefficient, longer mixing time, and lower carbon dioxide removal rate than was seen in smaller, bench scale bioreactors [32]. It is important that these factors are taken into consideration during the scaleup process.

Figure 2 shows the various mixing patterns that can induce hydrodynamic stress in a bioreactor [33]. Figure 3, which shows activity in a bioreactor, shows the correlation between hydrodynamic stress and Reynolds number [34]. As the flow velocity and mixing rigor increases, hydrodynamic stress also increases. As a result, the goal of our project is to create a soft biosensor that can reproduce the values in Figure 3, operating as a prescreening tool to analyze the hydrodynamic stress before scaleup.
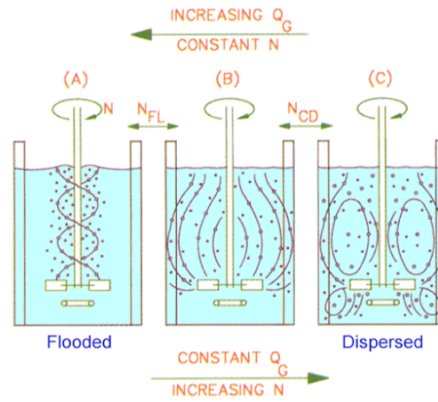
Figure 2. Mixing patterns in a bioreactor [33]. N: rpm of the propeller, Qg: gas flow rate.
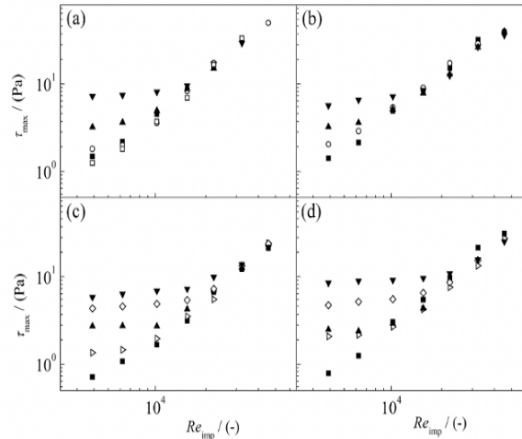
Figure 3. Graph of hydrodynamic stress vs. Reynolds number [34].

1.4.5 Flow Analysis

Monitoring of cell viability requires extraneous shear stress analysis for cells that have undergone an applied shear stress. The proportion of applied shear stress will correlate to the viability of the cells through numerous analyses. These analyses will include the use of the Navier-Stokes Equations, Newton's Law of Viscosity, the Reynolds number, and Bernoulli's Principle.

The Navier-Stokes Equations are partial differential equations that describe the flow of incompressible Newtonian fluids. The Navier Stokes equations are as follows:

$$\rho(u * \nabla)u = \nabla * [-\rho l + K] + F \ [1]$$

$$\rho\nabla * u = 0 \ [2]$$

$$K = \mu(\nabla u + (\nabla u)^T) \ [3]$$

u represents fluid flow, p represents fluid pressure, ρ represents fluid density, and μ represents fluid dynamic viscosity. F is the volume force vector, and $K = 0$ for non-viscous and incompressible flow. Equation 1 is a vector equation which represents conservation of momentum and Equation 2 is the continuity equation which represents the conservation of mass.

Newton's Law of Viscosity correlates the shear stress being applied and dynamic viscosity of the cellular solution [35]. Newton's Law of Viscosity is as follows:

$$\tau = \mu\frac{du}{dy} \ [4]$$

τ represents shear stress, which is interchangeable with hydrodynamic stress for the purposes of this project. μ represents viscosity and $\frac{du}{dy}$ is the rate of shear deformation.

The Reynolds number is important because it distinguishes between laminar and turbulent flow, explaining the relationship between velocity and associated shear. The Reynolds number is as follows:

$$Re = \frac{\rho VD}{\mu} \text{ [5]}$$

In this equation, ρ represents density, V represents velocity, D represents diameter, and μ represents bulk viscosity. It is important to ensure laminar flow of cells during our experiment, as if a proper laminar flow is not kept, then the proportionality of shear stress and flow rate cannot be correctly quantified [35].

Bernoulli's Principle describes the relation between pressure, velocity, and density in regard to flow. Bernoulli's Principle is as follows:

$$P_1 + \frac{1}{2}\rho V_1^2 + \rho g h_1 = P_2 + \frac{1}{2}\rho V_2^2 + \rho g h_2 \text{ [6]}$$

In this equation, P, V, and ρ represents the pressure, velocity, and density of the fluid, respectively. g is acceleration due to gravity. Bernouilli's Principle is a key component of cell flow analysis, as Bernoulli's Principle takes into consideration the changing cross-sectional areas and enables a complete understanding of the flow type that cells are experiencing as well as the pressure differences associated with changing cross-sectional areas [35]. This is especially important to our project due to the changing cross-sectional areas associated with the microneedle design.

1.5 Project Proposal

In order to create a soft biosensor that can be used as a prescreening tool to analyze hydrodynamic stress before scaleup, SolidWorks will be used to redesign the wound healing microneedle array to induce more hydrodynamic stress. This involves reducing the number of microneedles in the array, and increasing the scale of the device in order to extrude larger capsules.

Once the device has been fabricated using SLA, encapsulated cells will be extruded through the soft biosensor. Cell viability will be determined by categorical scoring and by using a lactate dehydrogenase (LDH) cytotoxicity assay. The process of extrusion and analysis of viability create a loop system (Figure 4) which will be repeated until the cells have died. The number of extrusion loops will then be correlated to cell viability by quantifying the hydrodynamic stress experienced by CHO cells. Finally, we will compare the published hydrodynamic shear values in industrial bioreactors to the shear stress measured in our experimental setup to verify our device.

Cell Flow analysis for shear stress and viability
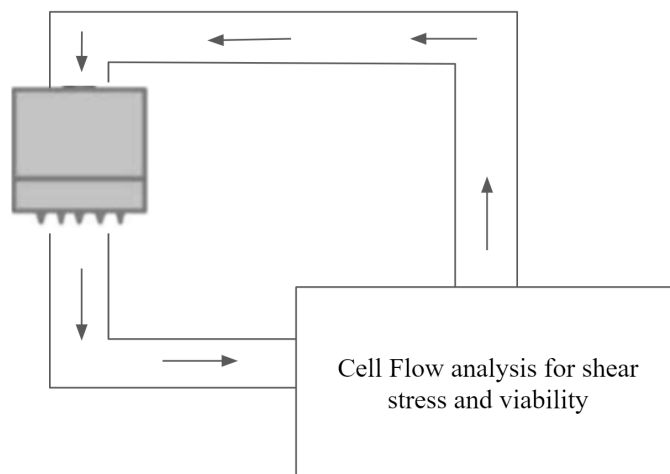
Figure 4. Diagram of extrusion loop workflow.

1.6 Importance

Overall, this project is important because our soft biosensor can be used to analyze the shear stress that microencapsulated CHO cells experience and apply this to high throughput screening applications. There is a need for large scale production of monoclonal antibodies to treat diseases such as cancer and Covid-19. Monoclonal antibody-based immunotherapy is a major component of cancer therapy, as these antibodies directly target tumor cells and promote continued anti-tumor immune responses [36]. Additionally, monoclonal antibodies such as bamlanivimab, etesevimab, casirivimab, imdevimab, and sotrovimab are being used to treat Covid-19 infection [37],[38],[39]. By measuring and understanding the hydrodynamic stress experienced by the encapsulated cells before each scaleup step, therapeutics such as monoclonal antibodies can be produced more efficiently, lowering the cost of these important drugs.

1.7 Project Aims

Our current aims for this project are the following:

1. Translate the design of the custom hollow microneedle array from a wound healing application to a high throughput scalable bioprocessing application.

2. Correlate the number of extrusion loops to cell viability by quantifying the hydrodynamic shear experienced by CHO cells.

Chapter 2: System Level

2.1 System Level Overview

The current design of the soft biosensors device is composed of two main parts: one containing the array of hollow microneedles, and the other consisting of a fluid chamber.

2.1.1 Simulation

COMSOL Multiphysics 5.6 was used to simulate the flow through the original wound healing microneedle array. Figure 5 shows that a very slow flow rate was needed in order for encapsulated cells to pass through all 13 microneedles. When the flow rate is increased, the flow is focused in the center of the array. Inducing shear involves higher flow rates, so this information prompted the creation of a 5 microneedle array for our soft biosensor device. In this design, the needles were enlarged and focused around the center of the array.

Therapeutic velocity
$V_1 = 1.6$ e-4 m/s

Bioprocessing Velocity
$V_2 = 1.6$ e-2 m/s
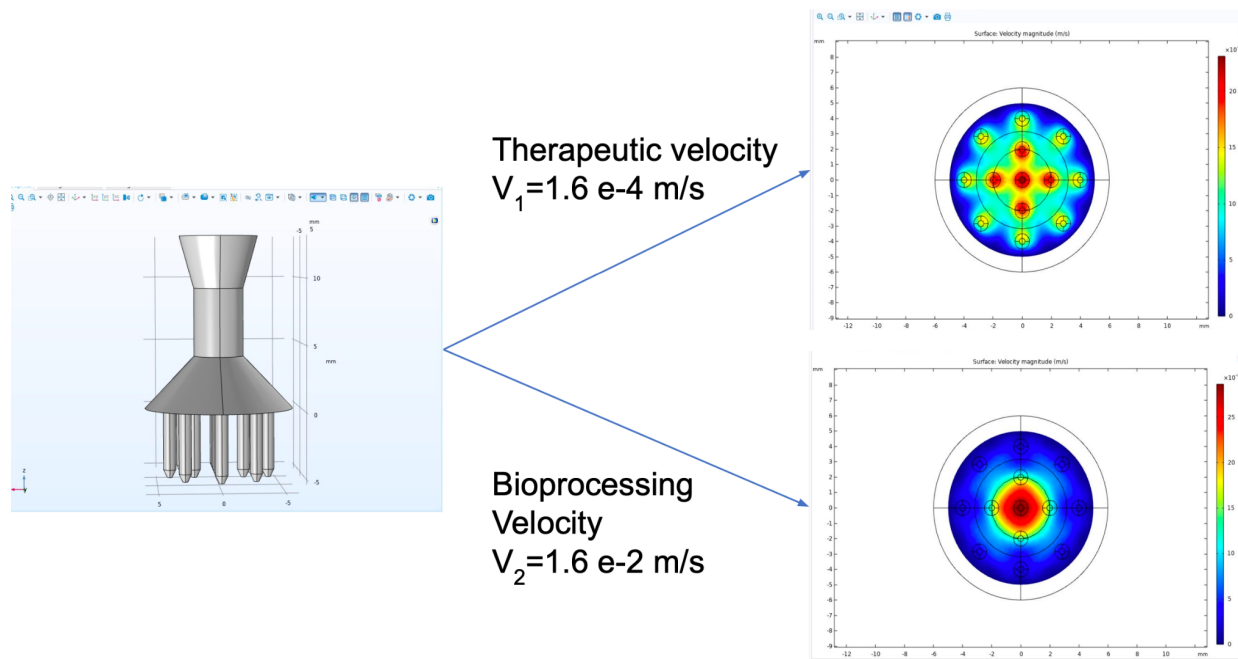
Figure 5. Comparison of therapeutic velocity and bioprocessing velocity through the wound healing microneedle array.

Our first simulation of flow was through a microneedle array in which the enlarged microneedles were placed inside the device. This was a precaution to ensure structural integrity and stability of the larger microneedles, as we worried that the heat from the 3D printer would cause the exposed microneedles to melt. In Figure 6, the hydrodynamic stress is 2 Pa, which is larger than the previous value of 1 Pa from the wound healing design. Additionally, we can see that the surface Reynolds Number is 35, which is in the laminar flow region.
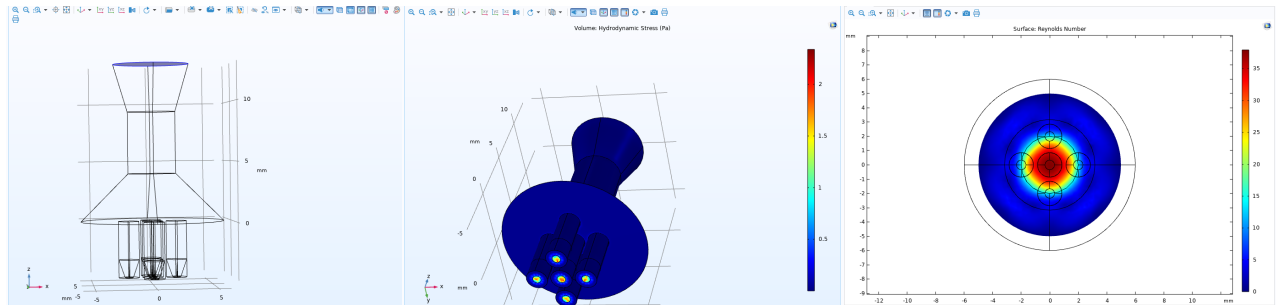
Figure 6. Simulation of flow through array with microneedles inside the device.
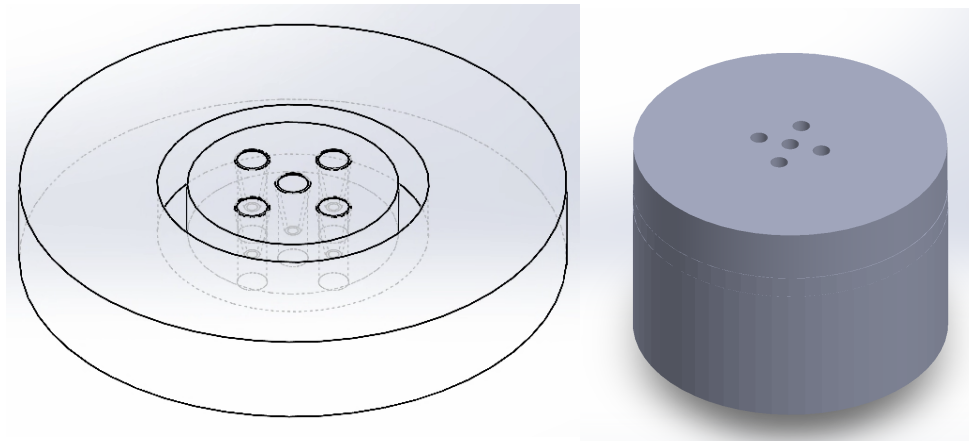
Figure 7. SolidWorks representation of soft biosensor with microneedles inside device.

For our second simulation of flow, the enlarged microneedles were placed on the outside of the device. This simulation (Figure 8) shows that the hydrodynamic stress has a maximum of 3.5 Pa, which is larger than the values associated with our first design. Additionally, the new design has a surface Reynolds Number of 350, which is an order of magnitude larger than the Reynold's

number value from our first design. This was our most successful design, as it induced the most shear and had the highest surface Reynolds number.
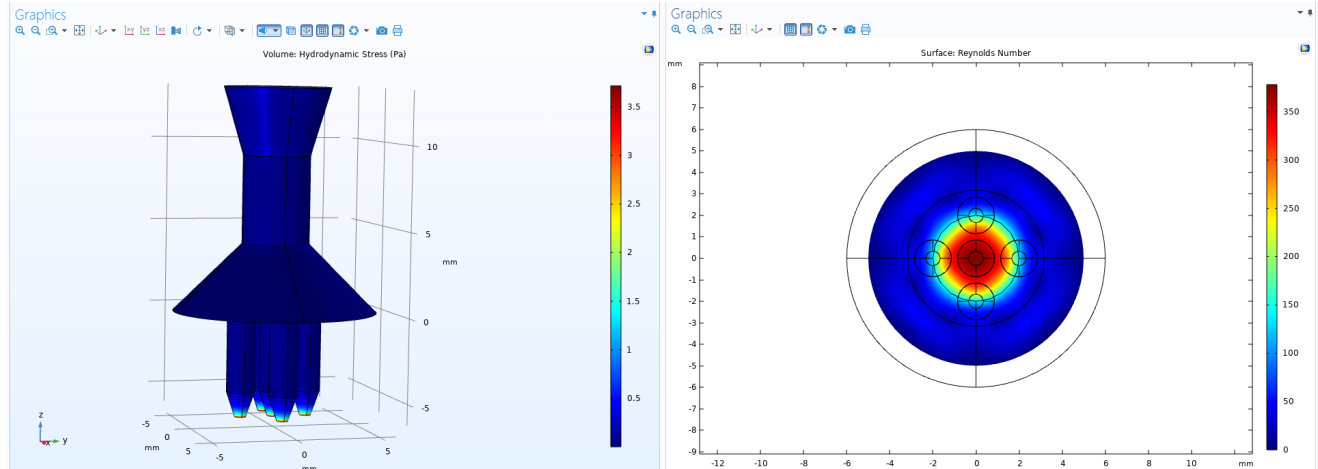
Figure 8. Simulation of flow through new microneedle array design.

2.1.2 Soft Biosensor Design

The bottom component of the device (Figure 9) is a circular surface with a diameter of 28.5 mm and a thickness of 4.72 mm. An array of 5 conical-shaped hollow microneedles are organized in a circular pattern on this surface. The dimensions of the cones are: 3 mm in height, a base diameter of 1.6 mm, and a tip diameter of 0.8 mm. These larger dimensions allow for larger microcapsules to pass through the needle and induce more shear. Additionally, the wall thickness was increased to 0.12 mm so that the longer microneedles were stable and secure after being 3D printed. This design can be scaled when 3D printing, which allows for this design to accommodate a variety of microcapsule sizes.

13
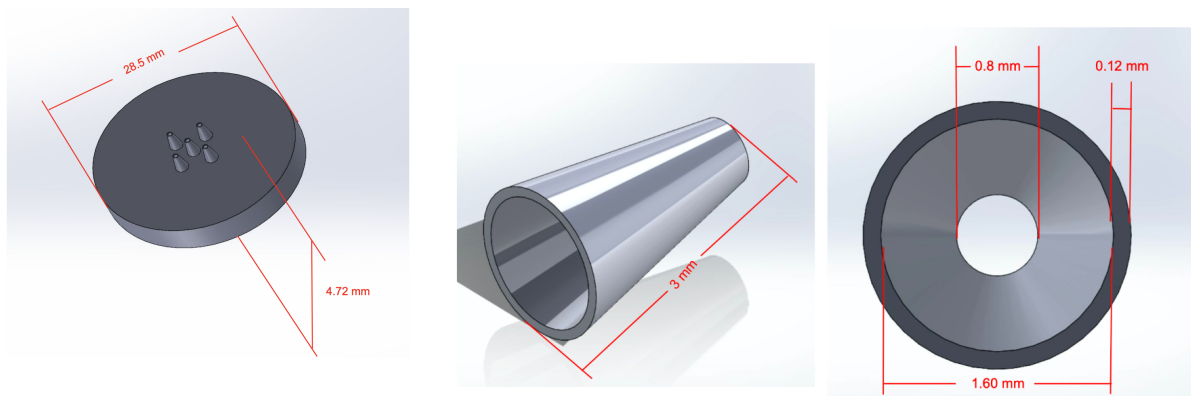
Figure 9. SolidWorks design of microneedle and microneedle array with dimensions.
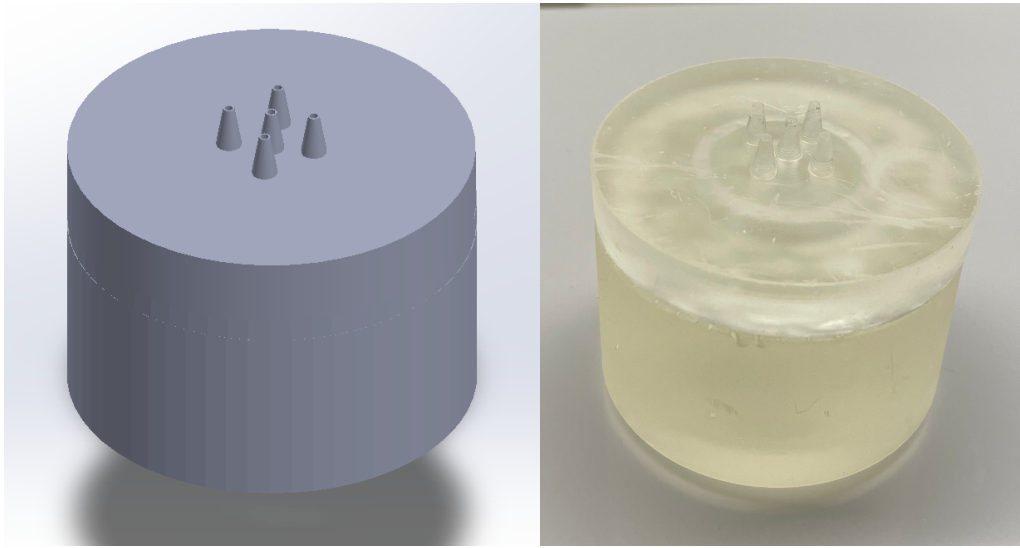
Figure 10. SolidWorks representation and 3D printed soft biosensor device.

2.2 System Level Requirements

Our system must be effective in inducing shear. This is the reason for our design change, as the larger needles resulted in higher values of hydrodynamic shear and surface Reynold's number, with the needles focused in the center of the device to allow for higher flow rates. Additionally, it is important that our device does not clog so that the encapsulated cells can be properly extruded and analyzed.

2.2.1 Benchmarking Results

No studies so far have used a hollow microneedles system as a prescreening tool for shear analysis. Our procedure will use lactate dehydrogenase as an indicator of shear. One study uses a droplet based microfluidic screening platform as a way to detect lactate dehydrogenase, and in turn shear stress [40]. This study involves using a screening assay and fluorescence to detect the levels of lactate dehydrogenase in encapsulated cells. Another study used chambers to augment and refine microfluidic devices to provide the opportunity to apply homogeneous shear stress to cells [41]. This study attempts to design an in-vitro device that can be used to apply physiologically relevant mechanical stress to a line of intestinal epithelial cells. The main

14

purpose behind their device was to induce differentiation for cells with the use of shear stress. This study exemplifies another method for introducing shear stress to cells in order to measure various components of cellular activity, which connects to the main objective of our project with similarities in inducing shear stress and analyzing cells.

In terms of analyzing hydrodynamic stress, one study created an aggregate breakup system, using contracting nozzles to convert the measured aggregate sizes into hydrodynamic stress [7]. The study found that the measured values of hydrodynamic stress agreed with literature data, supporting the applicability of their method to characterize the maximum effective hydrodynamic stress in complicated multiphase flow [7]. After further work, the same group developed a loop system to evaluate the maximum operating range for stirring, based on a maximum tolerable hydrodynamic stress in a bioreactor [8]. This study showed for the first time a validation study for a scale-down model, with their system allowing for a better understanding of the scaling process in bioreactors. While these studies analyze hydrodynamic stress during the scaleup process, no other study has attempted to use a 3D printed microneedle array, a low cost and accessible device, to analyze shear stress, making our approach a novel concept.

2.2.2 Functional Analysis
Our soft biosensor needs to execute the following functions:
- Allow for extrusion of 3 mm capsules
- Withstand multiple cycles of encapsulated cell extrusion
- Induce values of hydrodynamic shear that can be quantified

2.3 Team and Project Management
Our team is composed of two student members and our advisor. We maintained regular communication since the founding of our group and project, scheduling weekly meetings to discuss progress and next steps. All documents, such as literature search, photos, written work, and data analysis were uploaded to our shared Google Drive folder. Both group members are trained in Solidworks trained to work with mammalian cells.

2.3.1 Timeline

Table 2. 2021-2022 Project Timeline.

Fall 2021	Winter 2022	Spring 2022
● Literature research ● Define our problem ● Establish roles/execution plan ● Begin capsule fabrication	● Finalize device design ● Make functioning prototype ● Begin cell encapsulation and viability testing	● Complete testing ● Create Senior Design Presentation ● Write final thesis

2.3.2 Risks and Mitigation

A risk in our approach involves shrinkage occurring during 3D printing, as resin can shrink upon polymerization [42]. Because our soft biosensor consists of a top and bottom part that are glued together, shrinkage prevents the parts from fitting together properly. This can be mitigated by adjusting the dimensions of the bottom component and reprinting the part, as the design is flexible and can be edited in SolidWorks.

Chapter 3: Subsystems Levels
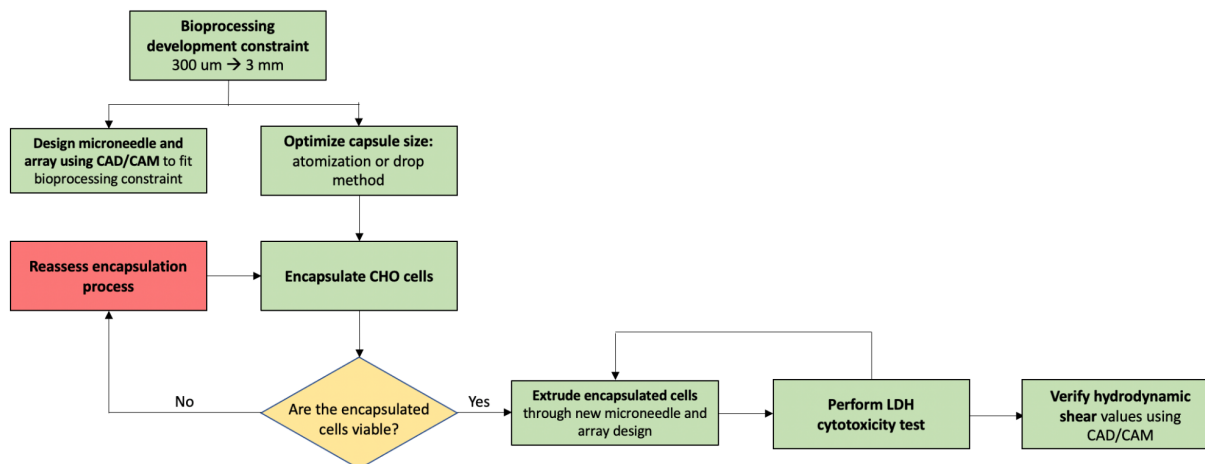
Figure 11. Subsystems flow chart.

3.1 Materials

In order to properly complete our project we needed an extensive list of materials. Our materials for this project include: Alginic Acid Sodium Salt from Brown Algae, Sodium Chloride, and Calcium Chloride Dihydrate were all obtained from Sigma Aldrich. Our Lactate Dehydrogenase (LDH) Cytotoxicity Assay was obtained from Thermo Fisher Scientific. The CHO cells, NE-1000 Channel Programmable Syringe Pump, coaxial needles, and sterile filters were all provided to us by the Santa Clara University Bioengineering Department.

3.2 Methods

3.2.1 Computation

Through computation, we were able to simulate and construct our adjustable and specified microneedle to fit the dimensions needed for properly experienced shear stress. Simulations were performed using COMSOL Multiphysics 5.6. These simulations mimicked flow rates through the microneedle, which allowed for the detection of proper and equal flow through each of the microneedles in our design, as well as a preview of the shear stress experienced by the material flowing through the microneedle at any given flow rate. Construction of the microneedle was done using SolidWorks. SolidWorks enabled a manipulative format for constructing the microneedle, allowing our microneedle to be flexible and easily adjusted.

3.2.2 Steam Sterilization

When working with cells, all of the materials used need to be properly sterilized to prevent any type of contamination during experimentation. In order to properly sterilize all of the materials, we used an autoclave. An autoclave is a machine that uses high temperatures and pressure to kill microorganisms and spores. The materials undergoing the sterilization included the alginate polymer, syringes, needles and solutions. Once autoclaved, the materials were safe to use for experimentation with the CHO cells.

3.2.3 Alginate Polymerization

The encapsulation of the CHO cells in the 3% alginate solution could only occur if the alginate is properly polymerized. In order to polymerize the alginate, we dropped the capsules into a 1.5% $CaCl_2$ solution. The $CaCl_2$ solution ionically interacted with the alginate, polymerizing it during the encapsulation process. Without this step, the capsules would not be able to take the spherical shape we needed in order to perform further analysis for cellular viability. Figure 12, below, shows how the $CaCl_2$ interacted with the alginate to polymerize it during the encapsulation process.
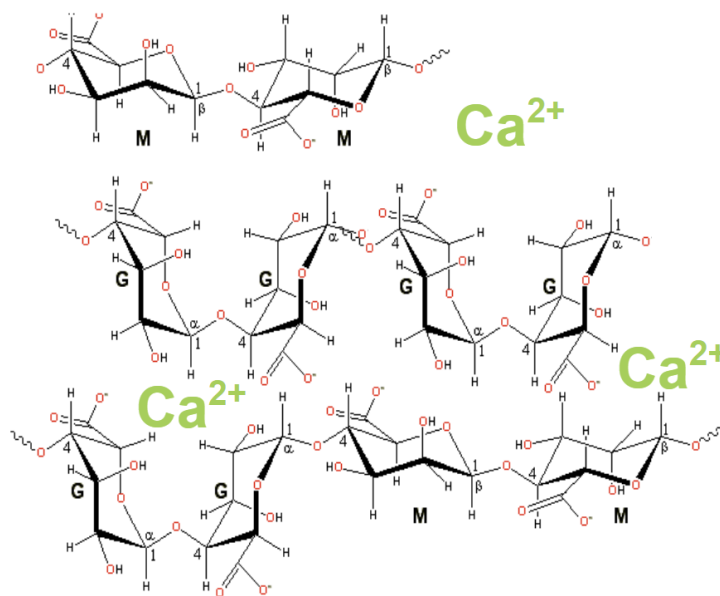
Figure 12. The polymerization of alginate through ionic interaction with the 1.5% $CaCl_2$ solution.

18

3.2.4 Light Microscopy

Light microscopy was used in parallel with the cytotoxicity assay as a way to visualize the CHO cells as they underwent encapsulation and viability testing. The specific microscope we used was the Leica DMI6000 B light microscope. Microscopy ensured the quality of our capsules in regard to shape and size, as well as the viability of the cells in terms of cell count and cell size. In addition, the microscope was capable of capturing images of our capsules and cells.

Figure 13. Leica DMI6000 B light microscope.

3.2.5 LDH Cytotoxicity Assay

This assay allows for measurement of cellular viability through an indirect measurement of extracellular LDH [43]. Extracellular LDH has been proven to be an adequate evaluation of cellular viability because the presence of extracellular LDH indicates a disruption in the membrane of the cell [44]. The direct measurement done by the assay is to measure the amount of red formazan formed. Red formazan is coupled with the LDH reaction, so the amount of red formazan directly correlates to the amount of extracellular LDH present.

Figure 14 shows the mechanism behind the cytotoxicity assay. Initially pyruvate reacts with LDH forming lactate and NAD^+ [45]. The NAD^+ then reacts with a different enzyme, diaphorase, which reacts with the tetrazolium salt to form red formazan, the molecule that can be analyzed through absorbance in spectrophotometry.
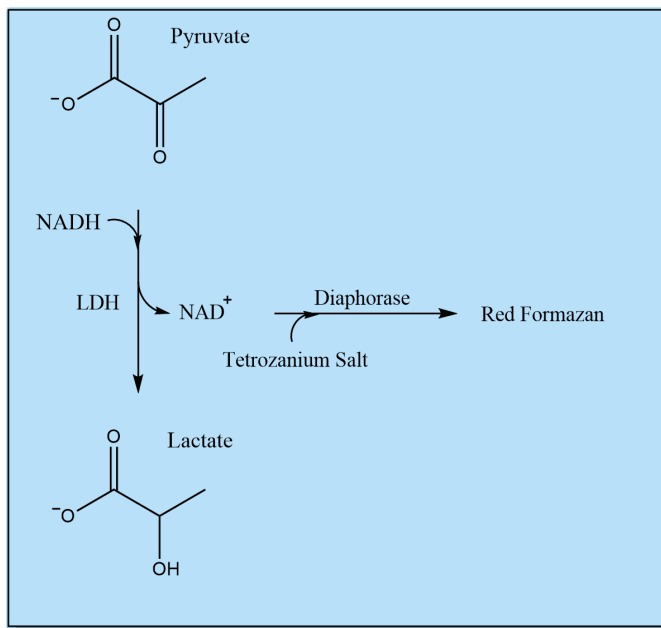
Figure 14. LDH cytotoxicity assay mechanism.

3.2.6 Statistical Analysis

The resulting absorbances from the cytotoxicity assays gave quantitative data for the viabilities of the cells. In order to analyze these values through a statistical analysis, we used a two sample correlated t-test on VassarStats [46]. Detecting any significant differences of the absorbance values between the three day testing period of the cytotoxicity assay was done using equations 7, 8, 9, 10 and 11.

$$S_d = \sqrt{\frac{n\Sigma_n d^2 - (\Sigma_n d)^2}{n^2(n-1)}} \ [7]$$

$$d \ = \ x_1 - x_2 \ [8]$$

$$x_1 \ is \ the \ first \ dataset$$

$$x_2 \ is \ the \ second \ dataset$$

$$\bar{d} = \bar{x}_1 - \bar{x}_2 \quad [9]$$

$$t = \frac{\bar{d}}{s_d / \sqrt{n}} \quad [10]$$

$$df = n - 1 \quad [11]$$

These equations allowed us a way to analyze p-values between absorbance from the three day testing period, securing our conclusion of significant differences in cellular viability.

Chapter 4: System Tests, Integration and Results

4.1 Experimental Procedures

4.1.1 Alginate Preparation

The hydrogel system is made up of brown algae mixed with 0.9% sodium chloride (NaCl) to make a 3% alginate solution. This solution would take 24 hours to make, needing constant mixture from a magnetic spinner between 400 - 500 rpm.

4.1.2 Cell Preparation

Cell preparation is needed to remove CHO cells from the culture plate so they can be added to alginate. The below protocol is for 100 mm plates.

Solutions used: cell media (DMEM + 1% FBS), Trypsin, PBS

Notice: Any materials that enter the hood will be sprayed with 70% EtOH. This includes cell plates, pipettes, solutions, hands, etc.

1. Warm the cell media, trypsin, and PBS in a 37°C water bath for 10 minutes.
2. Aspirate cell media from the plate.
3. Add 2 mL of trypsin to the plate. Incubate at 37°C for 5 minutes.
4. Return plate to the hood. Add 5 mL cell media to the plate. Pipette up and down to ensure all cells are removed from the plate.
5. Transfer contents of plate to a 15 mL conical centrifuge tube using a serological pipette and pipette controller.
6. Centrifuge at 3000 RPM for 1 minute.
7. Aspirate and resuspend pellet in 0.5 mL PBS.

4.1.3 Polyelectrolyte Complexation

Cell encapsulation includes encapsulating CHO cells in spherical 3% Brown Algae capsules. This process begins with the addition of the 500 mL pellet to 3 mL of the alginate, mixing this solution for 10 minutes. The alginate and CHO cell solution are then added to a 3 mL syringe

with a coaxial needle (Figure 15). The filled syringe and needle are secured to an NE-1000 Channel Programmable Syringe Pump, which allows for constant flow of the alginate and CHO cell solution through the syringe and coaxial needle. The syringe pump was set to run at a liquid flow rate of 1.0 mL/min. In addition to the pump, an air source would be connected to the coaxial needle, creating an air flow rate of 2.0 mL/min. The air source served as a way to cut the alginate inside of the needle allowing for the spherical capsules to form. As the alginate and CHO cell solutions moved through the needle, capsules were dropped into a 1.5% Calcium Chloride ($CaCl_2$) solution, where they sat for 20 minutes to crosslink. A standard needle was used to create 3 mm capsules (Figure 16).

Figure 15. Coaxial needle used to create 1 mm alginate capsules.

Figure 16. Standard needle used to create 3 mm alginate capsules.

4.1.4 LDH Cytotoxicity Assay

In order to perform the cytotoxicity assay, one capsule filled with cells was placed into each of 3 wells of a 96-well plate. PBS was added to 3 different wells as a negative control condition. The premade reaction mixture from the assay kit is added to the 6 wells, then the capsules and negative control incubate at 37 °C for 15 minutes. After 15 minutes, a stop solution from the assay kit is added to each well to halt any further LDH reactions. After the stop solution was added, the 96-well plate is placed into a spectrophotometer to record the absorbance values between 490 nm and 680 nm. Absorbance values quantified the amount of extracellular LDH present, which could then be used to determine the viability of the cells.

4.1.5 3D Printing

SLA was used to fabricate the soft biosensor device. The device was printed at 2x scale of the original file to accommodate the extrusion of larger capsules. After the part was 3D printed, it was washed in alcohol for 10 minutes, rinsed in DI water for 30 minutes, and UV cured for 5 minutes, but there is still room for this protocol to be optimized.

4.1.6 Compression Testing

Compression testing was completed to determine the mechanical strength of the 3mm capsules. 4 different conditions were tested:

1. Alginate capsules in saline at room temperature
2. Alginate capsules in saline at 37 °C
3. Alginate capsules in cell media at room temperature
4. Alginate capsules in cell media at 37 °C

Compression tests were performed using the BioMomentum Mach-1 Mechanical Testing System. First, the Find Contact function was used to position the 12.2mm diameter flat indenter. The conditions used are listed below:

Contact Criteria, gf: **1.500000**
Stage Velocity, mm/s: **0.2000**
Stage Limit, mm: **10.0000**

Stage Repositioning: Stop Criteria + Offset

Offset, mm: **0.2000**

Then, the Move Relative function was used to compress the capsules by 1.0 mm (33%) at a velocity of 0.5 mm/s. Microsoft Excel was used to analyze the compression data.

4.2 Results and Discussion

4.2.1 Printing Quality

Various dimension tests were performed to obtain the correct measurements so that our microneedles can withstand extrusion. Our original microneedle design had the same wall thickness as the 2018 design [9], an outer diameter D = 1.75 mm, and an inner diameter d = 0.70 mm. Figure 17a shows this design after 3D printing. These needles were extremely weak and flimsy, collapsing because the original wall thickness could not support the microneedles after 3D printing.

Therefore, we continued to redesign the microneedle until we found two dimensions that would be able to withstand the process of being 3D printed. Figure 17b has a wall thickness of 0.10 mm, D = 1.63 mm, and d = 0.60 mm. Figure 17c has a wall thickness of 0.12 mm, D = 1.6 mm, and d = 0.80 mm. Figure 17c is the final design, as the larger tip opening allows for larger capsules to be extruded and can induce more shear as compared to the design seen in Figure 17b.

(a)   (b)   (c)
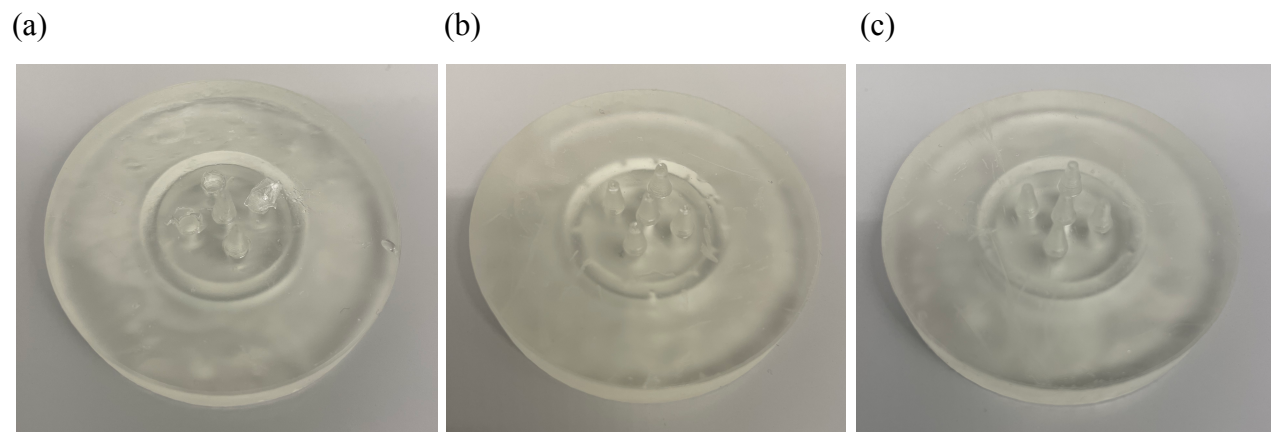
Figure 17a, b, c. Dimension tests of microneedle array. (**a**) Original wall thickness, outer diameter D = 1.75 mm, inner diameter d = 0.70 mm. (**b**) 0.10 mm wall thickness, D = 1.63 mm, d = 0.60 mm. (**c**) 0.12 mm wall thickness, D = 1.6 mm, d = 0.80 mm.

Table 3. Summary of Microneedle Revisions.

Design	Needle Height	Needle Thickness	Needle Base Diameter	Needle Tip Diameter
1	3 mm	Original	1.75 mm	0.70 mm
2	3 mm	0.10 mm	1.63 mm	0.60 mm
3	3 mm	0.12 mm	1.60 mm	0.80 mm

4.2.2 Cell Encapsulation

Figure 18 is a 1 mm alginate capsule with CHO cells. This capsule is more ideal for the previous wound healing application, therefore we redesigned the capsule itself to be much bigger at 3 mm in diameter (Figure 19). This larger size is much better for the high throughput bioprocessing application, as the larger size increases the hydrodynamic stress experienced during extrusion, more properly mimicking activity in industrial bioreactors.
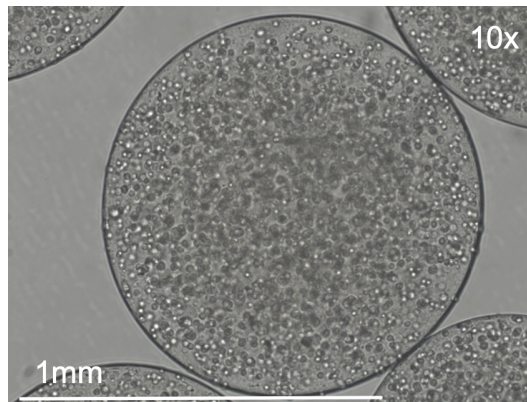
Figure 18. ~1 mm alginate microcapsules with cells. Image taken at 10x magnification.
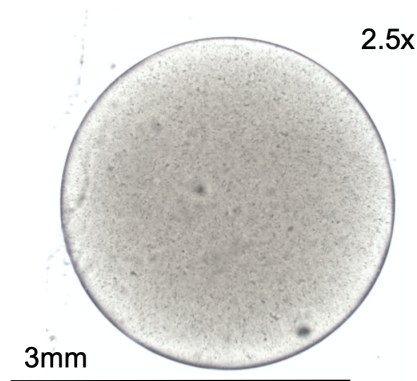
Figure 19. ~3 mm alginate empty microcapsules. Image taken at 2.5x magnification.

4.2.3 100% Confluency Experiments

In this experiment, the cell culture plate was 60% confluent prior to cell encapsulation.

4.2.3.1 Categorical Scoring of Viability

We assessed cell viability over a 3 day period. Cell viability can be categorically assessed by observing the increase or decrease in spheroid moieties throughout the capsule. Beginning on Day 0, Figure 20a shows alginate capsules containing the cells on the day of encapsulation. Figure 20b shows the capsules 1 day after encapsulation. The capsule has increased in size because of the absorption of cell media. The cells have also increased in size, meaning they are alive and maintaining cellular function. This trend continues on Day 2 (Figure 20c), as the capsules have increased in size and the cells multiplied within the capsule. However, on Day 3 (Figure 20d), there is a decrease in the number of spheroid moieties in the capsule, indicating cell death. Additionally, the color of the image changes, which was caused by the yellowing of media, another indicator that the cells have died. We believe the cells died due to a lack of nutrients that was caused by too much cell growth in the capsule.
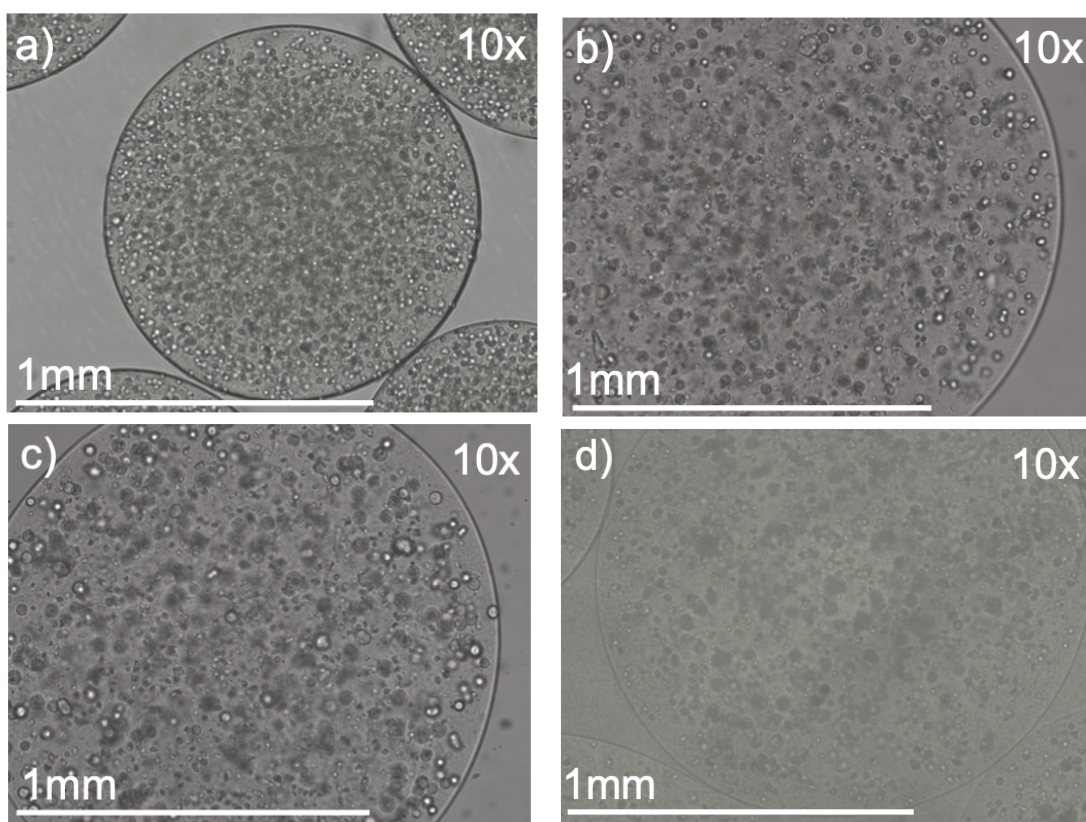
Figures 20a, b, c, d. Viability of encapsulated cells over 3 days (100% confluency). All images taken at 10x magnification. (**a**) Encapsulated cells on Day 0 (day of encapsulation). (**b**) Encapsulated cells on Day 1. (**c**) Encapsulated cells on Day 2. (**d**) Encapsulated cells on Day 3.

4.2.3.2 Cytotoxicity Assay

Cell viability is also determined using a cytotoxicity assay. Figure 21 shows LDH activity over the 3 day period. When looking at the average absorbance values, samples 2 and 3, as well as 1 and 3 have shown to be significantly different, resulting in a p-value of less than 0.001 from a t-test on VassarStats [46]. This indicated an increase in cell death on the third day as compared to the first and second days. This was in line with our results determined by visualizing our samples.
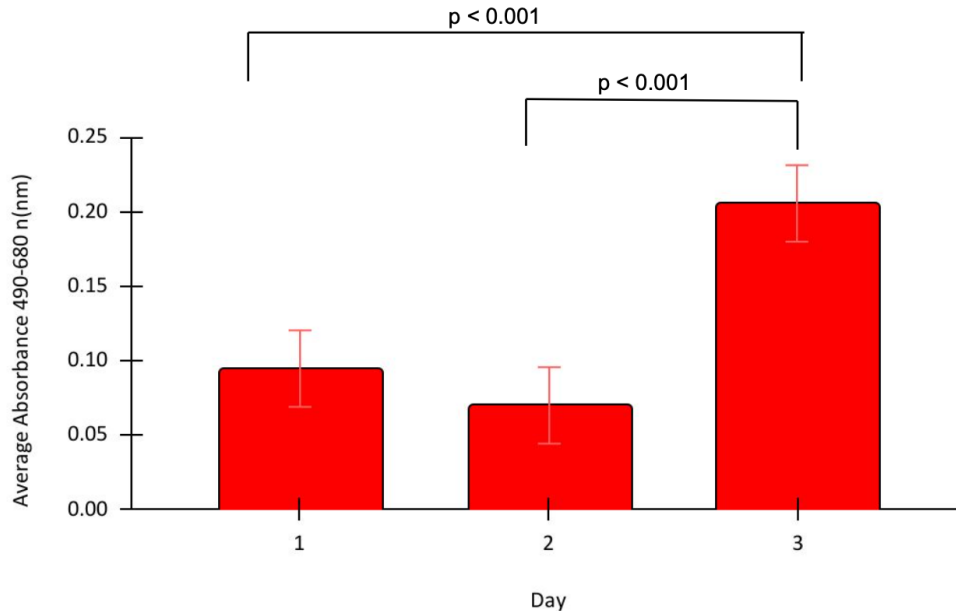
Figure 21. Average LDH activity over a 3 day period (100% confluency).

4.2.4 60% Confluency Experiments

After the encapsulated cells died on Day 3 of our previous cytotoxicity test, we performed another cytotoxicity test on encapsulated cells over a 3 day period. In this experiment, the cell culture plate was 60% confluent prior to cell encapsulation. We hoped that a less confluent plate would allow for cell survival up to Day 3.

4.2.4.1 Categorical Scoring of Viability

Beginning on Day 0, Figure 22a shows alginate capsules containing the cells on the day of encapsulation. Figure 22b shows the capsules 1 Day after encapsulation. The capsule has increased in size because of the absorption of cell media. The cells have also increased in size, meaning they are alive and maintaining cellular function. This trend continues on Day 2 (Figure 22c), as the capsules have increased in size and the cells multiplied within the capsule. On Day 3 (Figure 22d), showed a lack of spheroid moieties demonstrating a decrease in viability for the encapsulated cells . However, visually analyzing cell viability is more difficult with larger capsules, as the larger diameter makes it difficult to view inside the capsule.
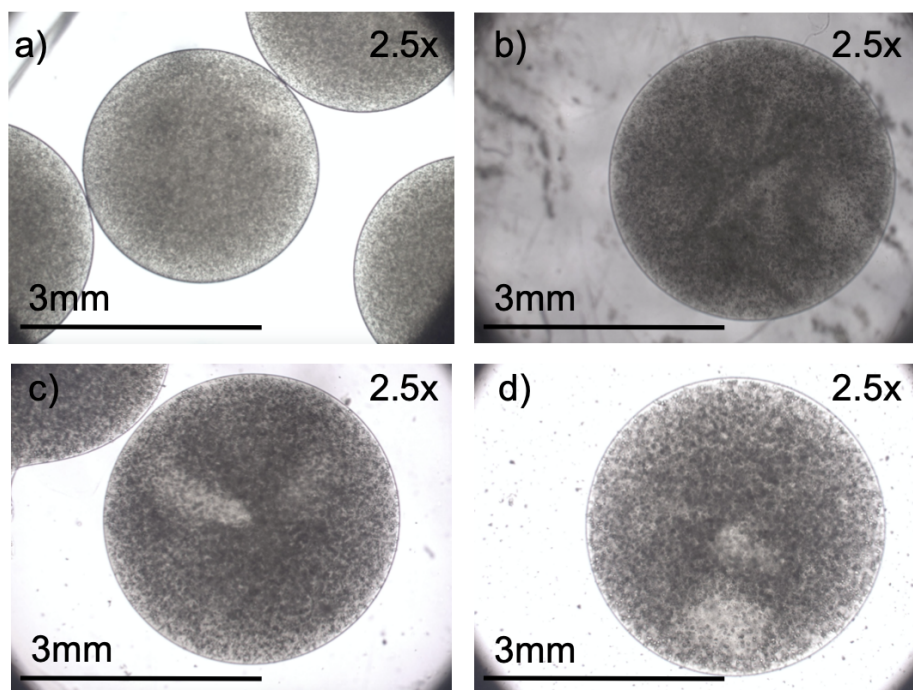
Figures 22a, b, c, d. Viability of encapsulated cells over 3 days (60% confluency). All images taken at 2.5x magnification. (**a**) Encapsulated cells on Day 0 (day of encapsulation). (**b**) Encapsulated cells on Day 1. (**c**) Encapsulated cells on Day 2. (**d**) Encapsulated cells on Day 3.

4.2.4.2 Cytotoxicity Testing

A second test on cell viability was also performed for a 3 day period, similar to the previous one. However, in this test, the cell culture plate was 60% confluent prior to cell encapsulation. In this cytotoxicity test, we again found a significant difference between the absorbance values on days 1 and 3 as well as Days 2 and 3 (Figure 23). The p-values between these days were both $p < 0.05$. The significance difference was calculated using the same t-test on VassarStats as previously mentioned. We expected the cells to die after dividing and increasing in size in the alginate capsules, lessening the amount of nutrients available, however, we hoped the less confluent plate would have survived through Day 3.
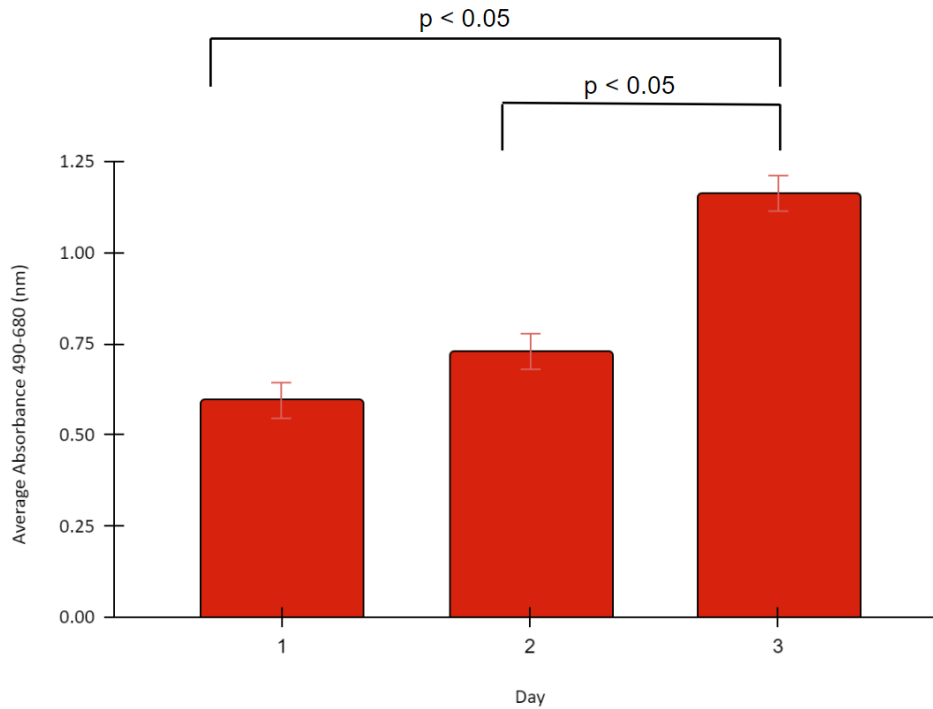
Figure 23. Average LDH activity over a 3 day period (60% confluency).

4.2.5 Compression Testing

Figures 24a, b, c, and d show the stress vs. strain graph of alginate capsules in saline at room temperature, alginate capsules in saline 37 °C, alginate capsules in cell media at room temperature, and alginate capsules in cell media at 37 °C, respectively. The elastic region of the stress vs. strain curve is defined by Hooke's Law:

$$\sigma \;=\; E\varepsilon \;[12]$$

The capsules in saline at room temperature have the highest Young's Modulus of 13.333 kPa. The capsules in cell media at 37 °C have the lowest Young's Modulus of 3.500 kPa. Because our capsules contain cells, they are placed in cell media at 37 °C for the cells to stay alive. This condition creates the softest capsules, which is important to note because the capsules must stay intact during extrusion. However, studies show that the average Young's modulus for 3 mm alginate beads ranged between 25–35 kPa [47]. In this way, this test must be repeated in order to determine the magnitude of the Young's Modulus.

(a)
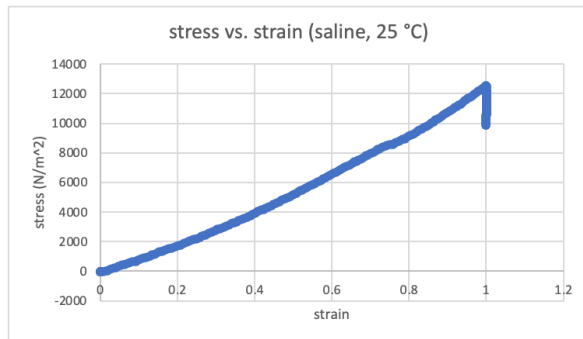
(b)
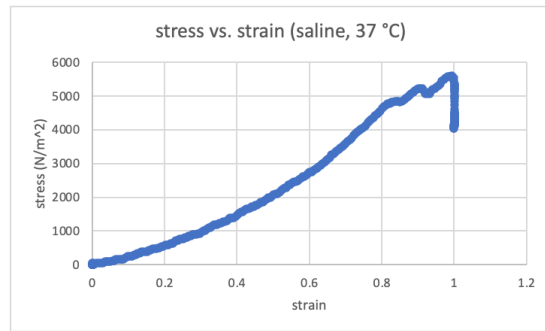
(c)
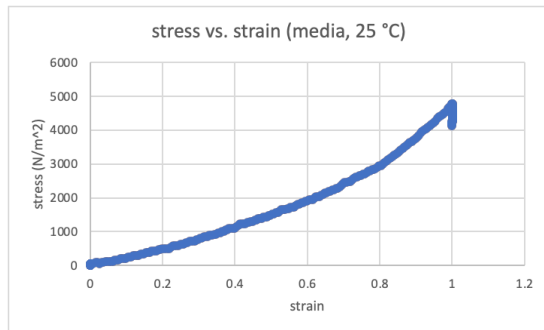
(d)
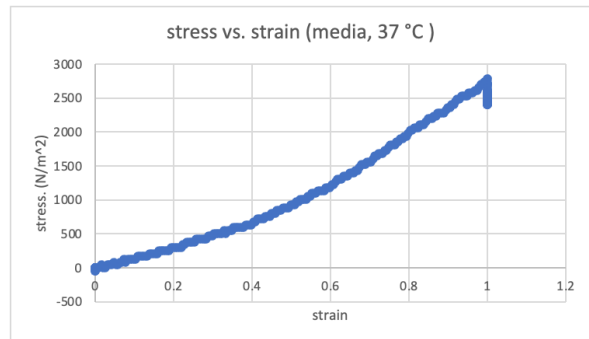
Figures 24a, b, c, d. Stress strain curves of alginate capsules in saline or cell media at room temperature (25 °C) or 37 °C. (**a**) Alginate capsules in saline at room temperature. (**b**) Alginate capsules in saline 37 °C. (**c**) Alginate capsules in cell media at room temperature. (**d**) Alginate capsules in cell media at 37 °C.

Table 4. Young's Modulus of Alginate Capsules.

$E_{\text{saline, 25 °C}}$	13.333 kPa
$E_{\text{saline, 37 °C}}$	8.333 kPa
$E_{\text{physiological, 25 °C}}$	8.000 kPa
$E_{\text{physiological, 37 °C}}$	3.500 kPa

Chapter 5: Cost Analysis

Table 5. Materials List and Costs.

Category	Materials	Vendor	Price
Encapsulation	Needles (custom x2)	N/A	**Provided by SoE**
Encapsulation	Syringe Pump	New Era Pump Systems	**Provided by SoE**
Encapsulation	3 mL BD Luer-Lok™ Syringe sterile, single use	BD	**$22.59**
Encapsulation	Algae, Sodium Chloride, Calcium Chloride	Sigma Aldrich	**Provided by SoE**
Cell Culture	CHO Cell line and cell culture materials	Department of Bioengineering	**Provided by BioE department (Zhang lab)**
Viability	LDH Cytotoxicity Assay Kit	Thermo Fisher	**$441**
Viability	96 Well Non-treated Plate with Lid, Individual, Sterile	CELLTREAT	**$178.06**
General Materials	100 μm Sterile Cell Filters Strainers (2 boxes)	Thermo Fisher	**Provided by SoE**
General Materials	Micropipette Tips	United Scientific Supplies	**$58.55**
General Materials	Sodium carboxymethyl cellulose	Sigma Aldrich	**$52.99**
Shipping	N/A	N/A	**$240.71**
TOTAL			**$993.90**

Our Project stayed within the budget of $1,000.

Table 6. Cost of Device.

Item	Cost
3D Printed Soft Biosensor	$12
Syringes	$1.13
TOTAL	$13.13

Chapter 6: Professional Issues and Constraints

6.1 Economic

From an economical standpoint, our project's purpose is to lessen the economic burden of the current industry bioreactors. If our system successfully maximizes cellular viability while the CHO cells undergo hydrodynamic shear stress, then there is potential for our system to be scaled-up to mimic large-scale bioreactors. Today, current bioreactors have been proven to cause cells to undergo an abundance of hydrodynamic shear stress causing a large amount of the cells within the bioreactors to undergo apoptosis or necrosis [48][49]. This is a huge waste of the biomaterials within the bioreactor, which accounts for the economic burden of current bioreactors. Our project offers the potential to lessen this burden and allow for an increase in biomaterial within bioreactors which then increases the amount of medical treatments manufactured for the population.

6.2 Health and Safety

Public health and safety needs to be a primary concern, especially when working with factors that can enable an increase of supply for varying medical treatments. This is even more important considering how COVID-19 has impacted the world, prompting the rapid production of large quantities of monoclonal antibodies to treat this epidemic. Monoclonal antibodies are also a significant aspect of cancer treatment. Therefore, we see that our project takes into consideration the importance of health and safety for the greater population throughout the world.

6.3 Manufacturability

The potential manufacturability of our project can prove to have some problems, just due to the prototypical aspects of our project at this stage. The system of the project would need to be further developed in order for manufacturability to increase. The system that we created is still within its early stages with regard to 3D printing, the process of cellular encapsulation and extrusion and viability testing through the cytotoxicity assay. As these aspects of the project are optimized our project would move more toward an increased ability of being manufactured at a large-scale.

6.4 Environmental Impact

As previously mentioned, the bioreactors seen today in the industry illustrate an abundance of hydrodynamic stress to cells, which increase the amount of apoptosis and necrosis of these cells. This results in a large amount of biological waste throughout the industry. This biological waste can have adverse effects on the environment because of the disposing of this waste. Lessening the amount of biological waste seen around the industry is a part of our project that would provide a positive impact to the environment. Another aspect of the project that contributes to the environment would be the water soluble chemistry related to the project. The disposal of the materials used in our project, such as sodium alginate, can be done through water solubility [50], having another positive impact on the environment.

6.5 Usability

Our microneedle system has been designed in a way that allows flexibility for varying applications. The microneedle design through the SolidWorks computation is readily available for changes in structures and design. Throughout our project we were able to manipulate the structures, widths, array layout, and heights of the microneedles at our discretion as we ran into various problems. However, this aspect is not only for troubleshooting, it also serves to add flexibility to the design of the microneedles associated with our system. This opens the door for other types of analysis in our system, including compression, cell-adhesion, temperature and pH analyses.

Chapter 7: Summary and Conclusions

7.1 Summary

The main objective of our project is to mimic the conditions experienced by industrial bioreactors by using a microneedle array system to create a soft biosensor. This device allows for the detection of shear stress experienced by cells within industrial bioreactors, and in doing this, we can maximize cellular viability for the cells experiencing the shear stress. Maximizing cellular viability in these high shear stress environments can have tremendous impact on the bioindustry by saving biomaterial used in bioreactors and increasing the production of various medical treatments such as cellular treatments, or monoclonal antibody production.

To begin our project, we first needed to develop a microneedle design that allowed for an adequate amount of experienced shear stress for the cells being extruded. We used SolidWorks to develop this design from the previously established custom microneedle system of the 2018 Senior Design Project "Three-Dimensional (3D) Printed Microneedles for Microencapsulated Cell Extrusion." Our design changes included increasing the size of the microneedles in terms of height, diameter, and thickness. We also change the array arrangement of the needles on the part from a 13 needle design to a 5 needle design. These changes allowed for an increase in shear stress to the cells being extruded, which is exactly what we needed to maximize cellular viability in the presence of shear stress. We were able to ensure the increased shear stress experienced during extrusion from the microneedle by simulating flow through a microneedle in COMSOL 5.6.

The next step for our project was polyelectrolyte complexation. This included encapsulating the CHO cells into a 3% alginate solution using an NE-1000 Channel Programmable Syringe Pump. This entire process required complete sterilization in order to prevent any type of contamination for the CHO cells. Sterilization was done by autoclaving each of the materials that would come into contact with the cells, including the alginate polymer, syringes, needles, glassware and solutions. Once the materials were properly sterilized, the cells were prepared using various techniques involving trypsinization and centrifugation. The cells were then added to 3 mL of alginate solution and mixed for 10 minutes. Once entirely mixed, the alginate solution would be

added to a 3 mL syringe connected to a coaxial needle, and the syringe would be placed in the syringe pump. The pump would then continually pump the alginate out of the syringe at a constant flow rate, allowing for spherical capsules to be formed. Cell filled alginate capsules were dropped from the syringe into a 1.5% $CaCl_2$ solution. The $CaCl_2$ solution polymerized the alginate, causing the capsules to gain robustness and sturdiness to maintain their spherical shapes.

Once the cells were encapsulated into alginate, we would begin our testing process of the cellular viability of the cells within the alginate. Upon encapsulation, light microscopy was used to visualize the cells. After 1, 2 and 3 days a cytotoxicity assay was performed to test the viability of the cells. Light microscopy allowed for the visualization of the cells and capsules to ensure the capsules were the correct size and shape, and that the cells were alive, dividing and growing. However, visualization was a quality check, whereas the cytotoxicity assay offered a more concrete quantity check by numerically evaluating the viability of the cells through absorbance values using a spectrophotometer. After the 3 day cytotoxicity assay analysis, the cells were properly disposed of through a series of bleaching and disposing into biohazardous waste containers.

7.2 Conclusion

In conclusion, we were able to successfully build the foundation of a prescreening system that enables further analysis of the effects of shear stress experienced by cells in industrial bioreactors. We developed a new microneedle structure, encapsulated cells in alginate, and tested the viability of the encapsulated cells. The microneedle design that we developed through 3D printing allowed for extensive analysis of the shear stress experienced by the encapsulated CHO cells when undergoing extrusion through the microneedle. This was proven through simulations done with COMSOL 5.6, showing the shear stress to be increased 3.5 times more than the previous microneedle design as well as an increase in the Reynolds number to 350. CHO cells were encapsulated in 3% algainte to create 3 mm capsules for extrusion through the soft biosensor, a size we found to adequately induce the proper amount of shear stress through an extrusion. The previous capsules were sized in the 1 mm range, and these were too small for our newer, and larger microneedle. A LDH cytotoxicity assay was used to analyze the viability of the

cells over a 3 day period following encapsulation. The results showed cell death to occur on day 3 with a $p < 0.001$ confidence (100% confluency) and $p < 0.05$ (60% confluency). Visualization of the encapsulated cells through light microscopy coincided with our cytotoxicity assay results with categorical analysis of the viability of the cells during this 3 day testing period. Finally, compression testing was performed on the 3 mm capsules to test their mechanical strength. The capsules Young's Modulus was found to be 2.7342 kPa. Overall, our device has the ability to induce shear stress with potential scalable opportunities, allowing for flexibility and manipulation for future work.

7.3 Future Work

Looking into the future, there can be many different approaches to optimizing our soft biosensor device. The varying methods have yet to be completely optimized, as cellular encapsulation and extrusion can be further developed into a more efficient and manufacturable system. Also, the 3D printing of the microneedle can also be optimized for large-scale production. Although our system has been developed to specifically analyze hydrodynamic shear stress, there are other potential applications that can be considered for analysis. For example, our project has the potential to expand to the analysis of compression, cell-adhesion, temperature and pH. Each of which have contributing factors to the usability of industrial bioreactors for development of varying medical treatments, including cellular treatments, antibody treatments and pharmaceutical treatments. We hope the future of our project dives into these potential applications in addition to a complete optimization of hydrodynamic shear stress experienced within bioreactors.

Chapter 8: References

[1] Curley, S.M., Nicoletti, S.E., & Sharfstein, S.T. (2019). 3.58 - Applications of Nanotechnology to Bioprocessing. In Moo-Young, M., *Comprehensive Biotechnology Third Edition* (pp. 712-730). Pergamon. https://doi.org/10.1016/B978-0-444-64046-8.00193-2.

[2] Ding, Y., Marino, M., Zen, K., Sheffer, J., Almaguer, N., Caddy, K., & Praseuth, A. (2020). Considerations for Monoclonal Antibody Bioprocess and Manufacturing Validation. Pharmaceutical Technology, 44(8), 31–36. https://www.pharmtech.com/view/considerations-for-monoclonal-antibody-bioprocess-and-manufacturing-validation.

[3] Lu, R.M., Hwang, Y.C., Liu, I.J. *et al.* (2020). Development of therapeutic antibodies for the treatment of diseases. *J Biomed Sci, 27*(1). https://doi.org/10.1186/s12929-019-0592-z.

[4] Agostinetto, R., Rossi, M., Dawson, J., Lim, A., Simoneau, M.H., Boucher, C., Valldorf, B., Ross-Gillespie, A., Jardine, J.G., Sok, D., Burton, D.R., Hassell, T., Broly, H., Palinsky, W., Dupraz, P., Feinberg, M., Dey, & A.K. (2022). Rapid cGMP manufacturing of COVID-19 monoclonal antibody using stable CHO cell pools. *Biotechnol Bioeng, 119*(2), 663-666. DOI: 10.1002/bit.27995.

[5] Stephenson, M., & Grayson, W. (2018). Recent advances in bioreactors for cell-based therapies. *F1000Research, 7*, F1000 Faculty Rev-517. https://doi.org/10.12688/f1000research.12533.1.

[6] Zhan, C., Hagrot, E., Brandt, L., & Chotteau, V. (2019). Study of hydrodynamics in wave bioreactors by computational fluid dynamics reveals a resonance phenomenon. *Chemical Engineering Science, 193*, 53-65. https://doi.org/10.1016/j.ces.2018.08.017.

[7] Villiger, T.K., Morbidelli, M., & Soos, M. (2015). Experimental determination of maximum effective hydrodynamic stress in multiphase flow using shear sensitive aggregates. Transport Phenomena and Fluid Mechanics, 61(5), 1735-1744. https://doi.org/10.1002/aic.14753.

[8] Neunstoecklin, B., Villiger, T.K., Lucas, E. *et al.* (2016). Pilot-scale verification of maximum tolerable hydrodynamic stress for mammalian cell culture. *Appl Microbiol Biotechnol, 100*, 3489–3498. https://doi.org/10.1007/s00253-015-7193-x.

[9] Farias, C, Lyman, R., Hemingway, C., Chau, H., Mahacek, A., Bouzos, E., & Mobed-Miremadi, M. (2018). Three-Dimensional (3D) Printed Microneedles for Microencapsulated Cell Extrusion. *Bioengineering, 5*(3), 59–85. https://doi.org/10.3390/bioengineering5030059.

[10] Quisling, S., Vestal, L., & Enstrom, A. (2021). Flow Visualization of Bolus Microcapsule Delivery through 3D Printed Microneedles. *Bioengineering Senior Theses*, 105. https://scholarcommons.scu.edu/bioe_senior/105.

[11] Roche. (2011). Cell Proliferation Reagent WST-1. Version 16. www.roche-applied-science.com.

[12] Yang, J., Liu, X., Fu, Y., & Song, Y. (2019). Recent advances of microneedles for biomedical applications: drug delivery and beyond. *Acta Pharmaceutica Sinica B, 9*(3), 469-483. https://doi.org/10.1016/j.apsb.2019.03.007.

[13] Prausnitz, M.R., Mitragotri, S., & Langer, R. (2004). Current status and future potential of transdermal drug delivery. *Nat Rev Drug Discov*, *3*, 115–124. doi: 10.1038/nrd1304.

[14] Ita, K. (2015). Transdermal Delivery of Drugs with Microneedles—Potential and Challenges. Olatunji, O., ed. *Pharmaceutics*, *7*(3), 90-105. doi:10.3390/pharmaceutics7030090.

[15] Li, Y., Zhang, H., Yang, R. et al. (2019). Fabrication of sharp silicon hollow microneedles by deep-reactive ion etching towards minimally invasive diagnostics. *Microsyst Nanoeng, 5*(41), https://doi.org/10.1038/s41378-019-0077-y.

[16] Borys, B.S., Dang, T., So, T. *et al.* (2021). Overcoming bioprocess bottlenecks in the large-scale expansion of high-quality hiPSC aggregates in vertical-wheel stirred suspension bioreactors. *Stem Cell Res Ther, 12*(55). https://doi.org/10.1186/s13287-020-02109-4.

[17] Elanzew, A., Sommer, A., Pusch-Klein, A., Brüstle, O., & Haupt, Simone. (2015). A reproducible and versatile system for the dynamic expansion of human pluripotent stem cells in suspension. *Biotechnol. J.*, *10*(10), 1589–1599. https://doi.org/10.1002/biot.201400757.

[18] Badenes, S.M., Fernandes, T.G., Rodrigues, Carlos A.V., Diogo, M.M., & Cabral, J.M.S. (2016). Microcarrier-based platforms for in vitro expansion and differentiation of human pluripotent stem cells in bioreactor culture systems. J*ournal of Biotechnology, 234*, 71-82. https://doi.org/10.1016/j.jbiotec.2016.07.023.

[19] Gasperini, L., Mano, J. F., & Reis, R. L. (2014). Natural polymers for the microencapsulation of cells. *Journal of the Royal Society, Interface*, *11*(100), 20140817. https://doi.org/10.1098/rsif.2014.0817.

[20] Lee, K. Y., & Mooney, D. J. (2012). Alginate: properties and biomedical applications. *Progress in polymer science*, *37*(1), 106–126. https://doi.org/10.1016/j.progpolymsci.2011.06.003.

[21] Charbonier, F., Indana, D., & Chaudhuri, O. (2021). Tuning Viscoelasticity in Alginate Hydrogels for 3D Cell Culture Studies. *Current protocols*, *1*(5), e124. https://doi.org/10.1002/cpz1.124.

[22] Gong, Z., Szczesny, S.E., Caliari, S.R., Charrier, E.E., Chaudhuri, O., Cao, X., Lin, Y., Mauck, R.L., Janmey, P.A., Burdick, J.A., & Shenoy, V.B. (2018). Matching material and cellular timescales maximizes cell spreading on viscoelastic substrates. *Proc Natl Acad Sci USA,*

115(12), E2686-E2695. DOI: 10.1073/pnas.1716620115.

[23] Charrier, E.E., Pogoda. K., Wells, R.G., & Janmey, P.A. (2018). Control of cell morphology and differentiation by substrates with independently tunable elasticity and viscous dissipation. *Nature Communications*, *9*(1). doi: 10.1038/s41467-018-02906-9.

[24] Sta. Agueda, J.R.H., Chen, Q., Maalihan, R.D. *et al.* (2021). 3D printing of biomedically relevant polymer materials and biocompatibility. *MRS Communications,* 11, 197–212. https://doi.org/10.1557/s43579-021-00038-8.

[25] Pituru, S. M., Greabu, M., Totan, A., Imre, M., Pantea, M., Spinu, T., Tancu, A., Popoviciu, N. O., Stanescu, I. I., & Ionescu, E. (2020). A Review on the Biocompatibility of PMMA-Based Dental Materials for Interim Prosthetic Restorations with a Glimpse into their Modern Manufacturing Techniques. *Materials (Basel, Switzerland)*, *13*(13), 2894. https://doi.org/10.3390/ma13132894.

[26] Dumont, J., Euwart, D., Mei, B., Estes, S., & Kshirsagar, R. (2016). Human cell lines for biopharmaceutical manufacturing: history, status, and future perspectives. *Critical reviews in biotechnology*, *36*(6), 1110–1122. https://doi.org/10.3109/07388551.2015.1084266.

[27] Lai, T., Yang, Y., & Ng, S. K. (2013). Advances in Mammalian cell line development technologies for recombinant protein production. *Pharmaceuticals (Basel, Switzerland)*, *6*(5), 579–603. https://doi.org/10.3390/ph6050579.

[28] Formlabs, Inc. (2022). The Ultimate Guide to Stereolithography (SLA) 3D printing. Formlabs.com.

[29] Formlabs, Inc. (2018). Stereolithography 3D Printing: From the 1980s to Now. Formlabs.com.

[30] Formlabs, Inc. (2022). Formlabs Stereolithography 3D Printers Tech Specs Quick Stats. Formlabs.com.

[31] Stephenson, M. & Grayson, W. (2018). Recent advances in bioreactors for cell based therapies [version 1; peer review: 2 approved]. *F1000Research* 2018, 7(F1000 Faculty Rev):517. https://doi.org/10.12688/f1000research.12533.1.

[32] Xing, Z., Kenty, B.M., Li, Z.J, & Lee, S.S. (2009). Scale-up analysis for a CHO cell culture process in large-scale bioreactors. *Biotechnology and Bioengineering, 103*(4), 733-746. https://doi.org/10.1002/bit.22287.

[33] Bioprocess Engineering: Basic Concepts.

[34] Neunstoecklin, et al. (2015). Pilot-scale verification of maximum tolerable hydrodynamic stress for mammalian cell culture. *Applied Microbiology and Biotechnology.*

[35] Tanzeglock, T., Soos, M., Stephanopoulos, G., & Morbidelli, M. (2009). Induction of Mammalian Cell Death by Simple Shear and Extension Flows. *Biotechnology and Bioengineering*, *104*(2), 360-370. https://doi.org/10.1002/bit.22405.

[36] Zahavi, D., & Weiner, L. (2020). Monoclonal Antibodies in Cancer Therapy. *Antibodies (Basel, Switzerland)*, *9*(3), 34. https://doi.org/10.3390/antib9030034.

[37] Dougan, M., et al. (2021). Bamlanivimab plus Etesevimab in Mild or Moderate Covid-19. *N Engl J Med,* 385, 1382-1392. DOI: 10.1056/NEJMoa2102685.

[38] O'Brien, M.P., et al. (2021). Subcutaneous REGEN-COV Antibody Combination to Prevent Covid-19. *N Engl J Med,* 385, 1184-1195. DOI: 10.1056/NEJMoa2109682.

[39] Gupta, A., et al. Early Treatment for Covid-19 with SARS-CoV-2 Neutralizing Antibody Sotrovima. N Engl J Med, 385, 1941-1950. DOI: 10.1056/NEJMoa2107934.

[40] Cedillo-Alcantar, D.F., Han Y.D., Choi, J, Garcia-Cordero, J.L., & Revzin, A. (2019). Automated Droplet-Based Microfluidic Platform for Multiplexed Analysis of Biochemical Markers in Small Volumes. *Anal Chem*, *91*(8), 5133-5141. DOI: 10.1021/acs.analchem.8b05689.

[41] Lindner, M., Laporte, A., Block, S., Elomaa, L., & Weinhart, M. (2021). Physiological Shear Stress Enhances Differentiation, Mucus-Formation and Structural 3D Organization of Intestinal Epithelial Cells In Vitro. *Cells*, *10*(8), 2062. DOI: 10.3390/cells10082062.

[42] Gross, B.C., Erkal J.L., Lockwood, S.Y., Chen, C., & Spence, D.M. (2014). Evaluation of 3D Printing and Its Potential Impact on Biotechnology and the Chemical Sciences. *Anal. Chem.*, *86*(7), 3240–3253. doi/10.1021/ac403397r.

[43] Thermo Fisher Scientific. (2022). CyQUANT™ LDH Cytotoxicity Assay. Thermofisher.com.

[44] Kumar, P., Nagarajan, A., & Uchil, P.D. (2018). Analysis of Cell Viability by the Lactate Dehydrogenase Assay. *Cold Spring Harb Protoc.*, *2018*(6). doi: 10.1101/pdb.prot095497.

[45] Holbrook, J. J., & Gutfreund, H. (1973). Approaches to the study of enzyme mechanisms lactate dehydrogenase. *FEBS letters*, *31*(2), 157-169.

[46] VassarStats. Two-Sample t-Test for Independent or Correlated Samples. http://vassarstats.net/.

[47] Ceccaldi, C., Fullana, S.G., Alfarano, C., Lairez, O., Calise, D., Cussac, D., Parini, A., & Sallerin, B. (2012). Alginate scaffolds for mesenchymal stem cell cardiac therapy: influence of alginate composition. *Cell Transplant, 21*(9), 1969-1984. DOI: 10.3727/096368912X647252.

[48] Rotenberg, M. Y., Ruvinov, E., Armoza, A., & Cohen, S. (2012). A multi-shear perfusion bioreactor for investigating shear stress effects in endothelial cell constructs. *Lab on a Chip*,

12(15), 2696-2703.

[49] Grilo, A.L. & Mantalaris, A. (2019). Apoptosis: A mammalian cell bioprocessing perspective. Biotechnology Advances, 37(3), 459-475, https://doi.org/10.1016/j.biotechadv.2019.02.012.

[50] Loureiro dos Santos, L.A. (2017). Natural Polymeric Biomaterials: Processing and Properties. *Reference Module in Materials Science and Materials Engineering,* Elsevier. https://doi.org/10.1016/B978-0-12-803581-8.02253-0.

Chapter 9: Appendix

9.1 Cytotoxicity Assay Ladder

Before using the LDH cytotoxicity assay to test the viability of our encapsulated cells, we performed a ladder to practice using the assay (and determine the optimum cell count for the assay?). Figure 25 shows the setup of our experiment. The top row is the ladder, with the cell concentration decreasing from left well to right well. The middle row is a negative control (PBS), and the bottom row is the positive control (provided by the assay kit). Analyzing the absorbance values (Figure 26) shows us that the well with the highest concentration of cells have the most cell death, which is expected.
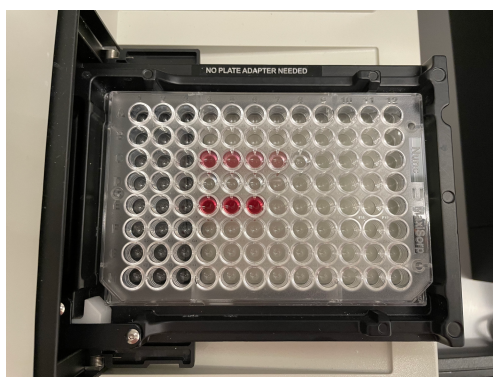

Figure 25. Cytotoxicity assay ladder setup. Top row: Ladder (concentration of cells from right well to left well: ladder (300 uL, 150 uL, 75 uL, 35 uL). Middle row: Negative control. Bottom row: Positive control.
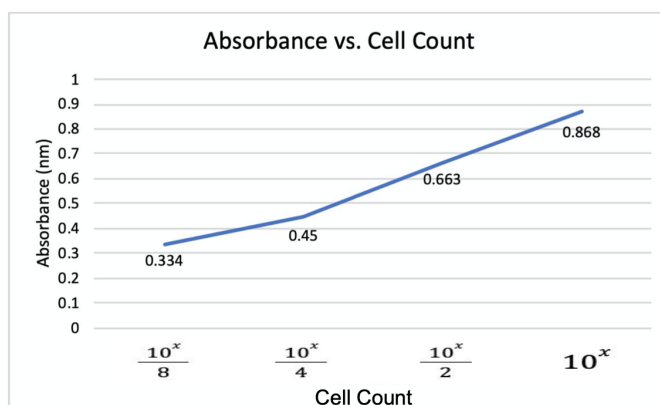

Figure 26. Plot of absorbance vs. cell count (to be replicated).